Alignment of Hg–Ar van der Waals molecule photofragments following photodissociation

C. J. K. Quayle, I. M. Bell, E. Takács,[a] X. Chen, and K. Burnett
Department of Physics, Clarendon Laboratory, Oxford, OX1 3PU, United Kingdom

D. M. Segal
Blackett Laboratory, Imperial College, London, SW7 2BZ, United Kingdom

(Received 4 August 1993; accepted 9 September 1993)

We have measured the alignment of the photofragments produced by photodissociation of Hg–Ar van der Waals molecules using light around 253.7 nm. The molecules are produced in the $X0^+$ ground state in a supersonic expansion. Tunable laser light close to the Hg 6 $^1S_0$–6 $^3P_1$ transition is then used to excite the molecule to the $B1^{\pm}$ state, in which it dissociates. The alignment of the resulting Hg($^3P_1$) asymptotic atoms is probed by tuning a delayed second laser to the 435.8 nm Hg 6 $^3P_1$–7 $^3S_1$ atomic transition and monitoring the subsequent fluorescence on the 7 $^3S_1$–6 $^3P_2$ transition around 546.1 nm. These measurements have been made, we believe for the first time, as a function of dissociating energy from very close to threshold to higher energies. The alignment shows a significant rise with increasing photon energy in line with a semiclassical picture of orbital locking at lower energies and rapid decoupling at higher energies. The results exhibit good agreement with the results of a fully quantum mechanical theory of the system.

I. INTRODUCTION

In recent years a wealth of experimental and theoretical data has been produced on photodissociation processes which result in anisotropic distributions or alignment of the photofragments.[1–5] The degree of alignment of the photofragment will, of course, depend critically on how the molecular orbitals evolve into atomic orbitals during the dissociation process, and one can therefore probe the molecular to atomic evolution through the measurement of photofragment alignment.

One gets the most from this method if the alignment can be measured as a function of dissociating photon energy over a range which extends from very close to threshold to higher continuum energies. This allows one to study a large variation in the kinetic energy of the relative motion of the photofragments, i.e., how the decoupling from molecular to atomic states depends on the speed of separation of the photofragments. Such measurements provide a good way to test the semiclassical "locking" models[6,7] that have been widely used to explain the results of experiments in studies of collisions and half-collisions. In this model the amount that the molecule rotates before decoupling to space fixed atomic states is critical. The degree of rotation depends, of course, on the amount of rotational energy that the molecule has and also on the time taken for the molecule to fully dissociate. If the photon energy is close to threshold, the speed of separation is low and the molecule has more time to rotate. As the photon energy is increased, however, the fragments fly apart faster and the molecule rotates less before decoupling. So as the dissociating laser is tuned above threshold we would expect to see an increase in the alignment, and therefore an increase in the observed polarization of the fluorescence.

Generally it is hard to find a system in which there is an appreciable cross section for dissociation close to threshold. One either has the problem of unfavorable Frank–Condon factors or lack of a suitable tunable laser source. For the case of the Hg–Ar van der Waals molecule, however, the discrete bound–bound vibrational transitions merge into a broad dissociation continuum for the $B1^{\pm}$ excited state.[8] This makes it possible to dissociate directly from the ground state to very close to the threshold for dissociation on the excited state. A further advantage of this system is that a great deal of work has already been performed on elucidating the Hg rare-gas potentials.[8–12] This has allowed a fully quantum-mechanical theoretical study of the Hg–Ar dissociation process to be carried out.[13] This experiment therefore provides a stringent test of these calculations.

The mercury transitions involved in this experiment and the route for dissociation of the Hg–Ar molecule into atomic fragments are shown in Fig. 1 along with the relevant potential curves. The large degree of spin–orbit coupling in mercury necessitates the use of a Hunds case-(c) basis at intermediate R, hence the labeling on the potentials. Tunable laser light close to the Hg 6s $^1S_0$–6p $^3P_1$ transition excites the molecule to the $B1^{\pm}$ state in which it dissociates. The alignment of the resulting Hg($^3P_1$) atoms is probed by using a delayed second laser which is tuned to the Hg 6p $^3P_1$–7s $^3S_1$ line and detecting the fluorescence on the 7s $^3S_1$–6p $^3P_2$ transition around 546.1 nm. The alignment of the excited atoms is often determined via the polarization of the re-emitted atomic fluorescence directly back down to the ground state so we relate our measurements to this polarization to enable comparison with other authors. With detection orthogonal to the direction of propagation of the lasers this information can be extracted from the ratio of the laser induced fluorescence (LIF) on the 7s $^3S_1$–6p $^3P_2$ transition for different polarizations of

[a]Present address: National Institute of Standards and Technology, Physics Building, A167 Gaithersburg, MD 20899.

 0021-9606/93/99(12)/9608/8/$6.00

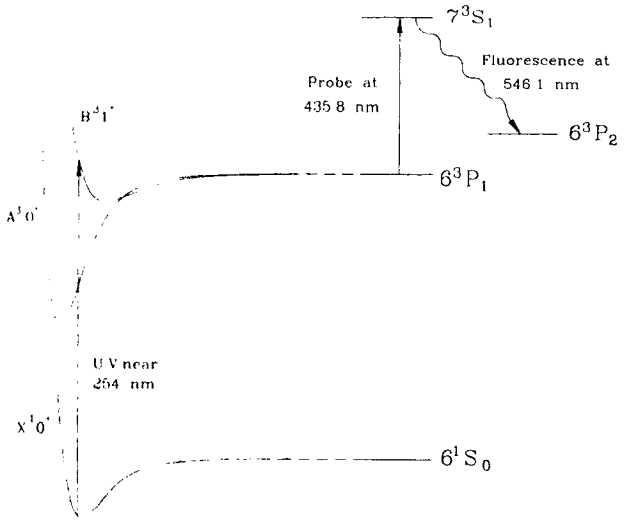

FIG. 1. Hg–Ar interatomic potentials of Segal and Harris together with the excitation scheme for the experiment. The UV laser causes excitation to the repulsive wall of the B state and hence dissociation. The asymptotic atoms are then probed by a second laser to a higher transition.

the UV laser. This two-step excitation scheme has been used previously and is superior to a single-step experiment in terms of maximizing the signal level and minimizing secondary depolarizing processes. These details are described in a previous paper.[14]

The rotational temperature of the molecules created in the beam is of the order of a few kelvin. This necessarily results in rotational states above the $J_i=0$ ground state being populated. One of the aims of the experiment is to dissociate these higher lying rotational states close to the dissociation energy for these states, however this energy will lie below the dissociation threshold of the $J_i=0$ state. Therefore when dissociating the higher lying states with photons of lower energy we will run the risk of exciting those molecules in the ground rotational state to high lying *bound* states, correlating with the asymptotic Hg $7s\,^3S_1$ state. If the fluorescence from these bound states is subsequently detected along with fluorescence from the asymptotic atoms, then there will be a significant reduction in the polarization measured.

Avoiding the contamination of the alignment with contributions from bound states is one of the most significant advantages of the two-step detection scheme. First, this is because probing the asymptotic atoms with the second laser acts as a narrow bandwidth detector, full width at half-maximum (FWHM) of 0.4 cm^{-1}. This effectively filters out detection of any bound states that lie outside the laser bandwidth. Second there is the fact that the line strength of an individual bound–bound molecular transition is much smaller than the corresponding atomic transition. This means that when the UV laser is dissociating high J_i states close to threshold, and therefore exciting the low J_i states to high lying bound states, the probe laser will preferentially excite the asymptotic Hg atoms rather than the bound states. This will, of course, only be the case if the response to the probe laser is linear on the atomic Hg

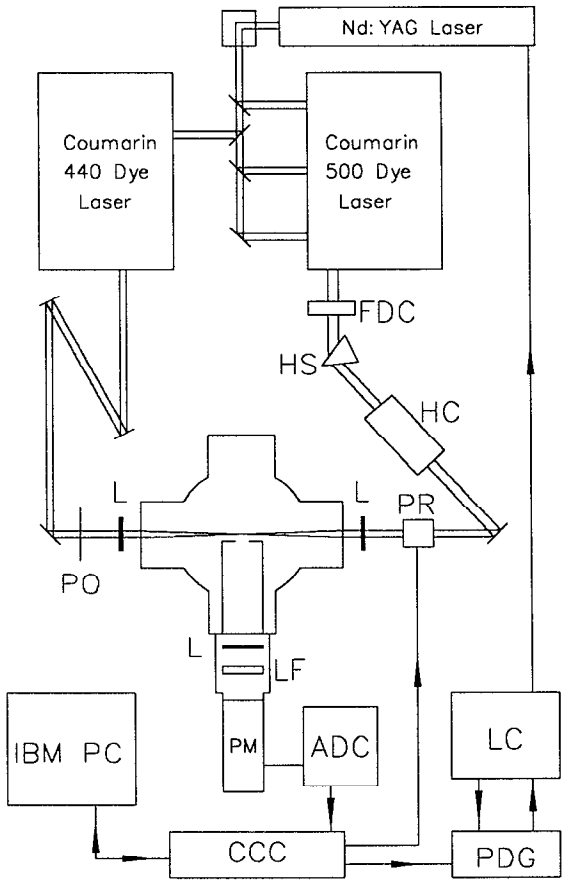

FIG. 2. Schematic representation of the experiment. CCC—CAMAC crate controller, PDG—pulse delay generator, LC—Nd:YAG laser controller, ADC—analogue to digital converter, PM—photomultiplier, FDC—frequency doubling crystal, HS—harmonic separator, HC—hot cell, PR—polarization rotator ($\lambda/2$ plate), PO—polarizer, LF—mercury green line filter, L—lens, EC—expansion chamber.

$6\,^3P_1$–$7\,^3S_1$ transition. This was ensured during the experiment by insertion of neutral density filters into the probe beam to the point where the linearity condition was satisfied.

In this paper we shall describe this experiment to measure the alignment as a function of dissociating photon energy and present the results for different initial rotational distributions of the molecules. The variation in alignment will be interpreted first in terms of semiclassical pictures of the dissociating process and then compared with the predictions of a quantum mechanical calculation that has been carried out for the system.

II. EXPERIMENT

A. Experimental details and procedure

The experimental apparatus is shown schematically in Fig. 2. Light close to the Hg $6s\,^1S_0$–$6p\,^3P_1$ line is produced using a dye laser configured as follows. The output of a Littman-type oscillator[15] with an intracavity beam expander using Coumarin 500 dye is amplified before being frequency doubled in a BBO crystal. Light at 435.8 nm is produced by a similar oscillator using Coumarin 440 dye.

The typical output of the lasers are 1 μJ in the UV and 30 μJ in the blue, and the pulses are approximately Gaussian in time with pulse lengths of the order 5 ns (FWHM) for the blue laser and 4 ns for the UV laser. Both dye lasers are pumped by the third harmonic of a commercial Nd:YAG laser running at 10 Hz repetition rate.

The experimental chamber is a six-armed stainless steel cross piece of total length 30 cm with arms of diameter 15 cm. The laser beams are arranged to counterpropagate in the cell and are focused to beam waists of 100 μm. Before entering the expansion chamber the UV passes through a heated quartz cell containing mercury to remove any frequency doubled amplified spontaneous emission (ASE) on the line center, which would otherwise cause excitation of free Hg atoms in the beam. The UV light leaves the frequency doubling crystal vertically polarized but is passed through a motor driven $\lambda/2$ plate before entering the chamber, which allows the polarization to be made alternately horizontal and vertical every 50 laser shots. The polarization of the blue laser is kept vertical by means of a crystal polarizer with a rejection ratio of 10^5.

A delay of about 5 ns is inserted in the blue laser line to ensure that the Hg atoms are not probed by the 435.8 nm light before all the dissociation events are complete. It is, however, desirable to keep this delay to a minimum to maximize signal and minimize the effects of any secondary depolarizing mechanisms (see Sec. II C). The Hg–Ar van der Waals molecules are produced in a cw supersonic expansion where pure argon at 2 bar is passed over mercury heated to 450 K before being expanded into a vacuum through a small nozzle. In the experiment two nozzle sizes were used to create a variation in the rotational temperature of the molecules formed.

The fluorescence from the $Hg(7s^3S_1)$ state is collimated by a 2 cm diam $f=20$ cm quartz lens before being passed through 546.1 nm line filter, with 10 nm bandpass, and on to the cathode of a photomultiplier. The signal for each laser shot from the photomultiplier is collected in a gated analogue to digital converter (ADC). The synchronization of the ADC with the laser pulse is achieved using a pulse delay generator controlled from an IBM PC which also collects and stores all the data from the ADC via a Transiac CAMAC crate controller.

B. The supersonic expansion

Miller[16] has calculated expressions for the flow field properties, i.e., temperature, pressure, and velocity for the center line of a three-dimensional free jet. The assumptions that the gas is ideal and that the flow is isentropic are expected to be good approximations for high speed flow. The results predict that the temperature, pressure, and collision frequency decrease rapidly just downstream of the nozzle and then reach a fairly stable regime after a few nozzle diameters. The temperature in this regime is predicted to be of the order of 1 K. This final temperature is dependent on the stagnation temperature and the nozzle diameter.

The usual reason for using supersonic expansions is to create an environment which is as cold and as collision free as possible. For this reason the beam is usually probed some way downstream from the nozzle where the gas has "frozen out"[16] to its coldest state. However in our experiment we wanted to be able to vary the initial rotational temperature of the molecules to allow monitoring of the alignment as a function of dissociation energy for *different* initial rotational states. To achieve this variation in initial temperature two nozzle diameters were used, one with a 150 μm diam pinhole to produce a fairly cold source and one with a 350 μm diam pinhole to produce a somewhat warmer one. Data were also taken for each nozzle at two different positions downstream of the nozzle: at 2 and 5 mm to create a further variation in temperature. Yamanouchi *et al.*[9] were able to rotationally resolve the spectra of Hg–Ar molecules produced in a similar expansion and were able to give an estimate of the beam rotational temperature by fitting their experimental data to theoretical predictions. This was determined to be 3.2 K whereas that found using Miller's results for their system is 0.9 K. This deviation from the predictions of continuum mechanics is attributed to the fact that the collision rate becomes too low to continue the process of cooling of the internal states which have therefore frozen out at the higher temperature. Consequently we expected the temperatures for the four cases where data has been taken to be higher than predicted in the range of a few kelvin.

C. Secondary depolarizing processes

There are several processes that reduce the initial alignment following dissociation. These processes obscure the observation of the nascent alignment after dissociation and so corrections must be made for them where possible. These depolarizing mechanisms are: (1) hyperfine structure, (2) Hanle effect, (3) collisions, and (4) radiation trapping. These have been discussed in the context of a previous polarization monitored collisional redistribution experiment[14] in Hg which used the same two-step pump–probe method of data collection. In the present case the Hanle effect and radiation trapping have a negligible effect on the polarization observed as in the collisional redistribution case and the reader is referred to Ref. 14. The situation is different, however, for depolarization due to hyperfine structure and second collisions, and these will be discussed below.

1. Hyperfine structure

When the molecule dissociates, it produces an excited Hg atom with a given alignment in the J, M_J representation. After the collision, recoupling of the M_I, M_J basis to F, M_F occurs under the influence of the hyperfine interaction. This leads to alignment being transferred from the electronic to the nuclear coordinates. The polarization of the resonance fluorescence, observed from the unresolved hyperfine multiplet, is therefore reduced. This is a well-known effect.[17,18]

In our experiment we probe the excited state rather than observing the fluorescence from it, and in doing so we partially resolve the hyperfine structure. Consequently when we tune the probe laser to maximum signal we are

predominantly tuning to a group of $I=0$ components and only weakly probing the many of the $I\neq 0$ components which lie outside the bandwidth of the probe laser. For the purpose of analysis the hyperfine structure must be treated as being resolved. This situation has previously been considered.[19,20] The alignment in the resolved hyperfine level is found to be reduced in comparison to that in the uncoupled (I,J) level. Relating the fluorescence ratio to alignment is therefore quite complicated, as the excitation of each hyperfine component from the $6\,^3P_1$ level to the $7\,^3S_1$ level has to be considered as well as the radiation pattern of the subsequent fluorescence. We have adapted the formalism of Greene and Zare[21] for the probing of product alignment by LIF to deal with this situation. A complete calculation will be presented separately.[22] In this paper we shall merely use the results of that analysis. Due to the fact that we are now predominantly probing $I=0$ components, which cause no depolarization, the reduction in the polarization due to the presence of $I\neq 0$ components is small, at around 7%.

2. Collisional depolarization

One of the reasons behind the widespread use of molecular beams in spectroscopy is their ability to produce cold and collision free environments. While the collision rate in the beam is indeed low it is still finite and becomes more significant in the higher temperature regions closer to the nozzle. In these regions the excited state atom, produced by photodissociation, will have a finite probability of experiencing a collision with a rare gas atom before the arrival of the probe laser. This will cause a reduction in the alignment measured at a time $t=t_d$ compared with that which would have been measured immediately after dissociation. The alignment $\alpha^{(2)}$ of the atom is related to the polarization of the fluorescence by the following expression

$$\alpha^{(2)}=\frac{2P}{3-P}. \tag{1}$$

As a result of collisions the alignment decays exponentially[23] with the time constant, $\gamma_c^{(2)}$, given by

$$\gamma_c^{(2)}=n_p\langle v\sigma^{(2)}\rangle. \tag{2}$$

Here v is the relative speed of the atom–perturber pair, n_p is the number density of perturbers, and $\sigma^{(2)}$ is a cross section for the destruction of alignment. The $\langle\cdots\rangle$ denotes an average over relative speeds and impact parameters. This allows us to calculate the alignment after a time t_d, the delay time between the two laser pulses, has elapsed, thus

$$\alpha^{(2)}(t_d)=\alpha^{(2)}\exp(-\gamma_c^{(2)}t_d). \tag{3}$$

The final amount of alignment observed in the pump–probe method is, therefore, dependent on the perturber pressure and the delay between the lasers. Taking the natural logarithm of Eq. (3) gives

$$\ln[\alpha^{(2)}(t_d)]=-\gamma_c^{(2)}t_d+\ln(\alpha^{(2)}). \tag{4}$$

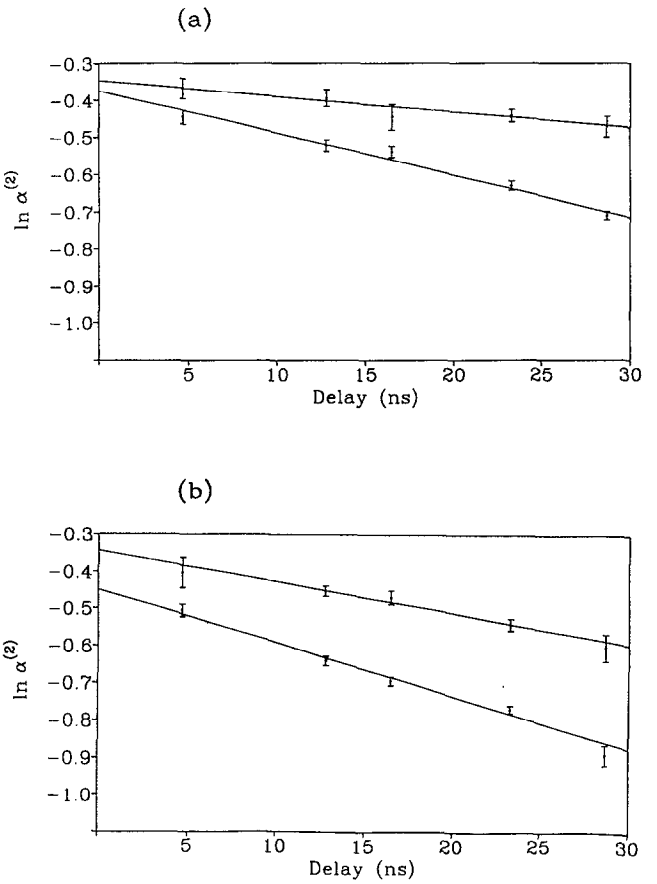

FIG. 3. Variation of the log of atomic alignment, $\ln(\alpha^{(2)})$, with the delay between the lasers together with best fit lines illustrating the linear dependance on laser delay. (a) and (b) show the data for the 150 μm nozzle and for the 350 μm nozzle, respectively, each probed at 5 mm (upper line) and 2 mm (lower line) downstream of the nozzle.

A plot of $\ln[\alpha^{(2)}(t_d)]$ against t_d will then yield a straight line, as shown in Fig. 3, allowing $-\gamma_c^{(2)}$ to be determined from the slope of the line.

In previous collisional redistribution experiments[14,24,25] carried out at pressures where depolarization due to collisions is significant, the quantity $\gamma_c^{(2)}$ was determined from a plot of polarization against perturber pressure. In the case of the molecular beam, however, we are not able to accurately measure the density in the supersonic region of the expansion, so an alternative method of finding $\gamma_c^{(2)}$ is required. This has been done by measuring the polarization as a function of the laser delay t_d. Figure 3 shows the data from the delay experiment. As predicted by Eq. (4) the plot exhibits a straight line, allowing a value of $\gamma_c^{(2)}$ to be calculated for each combination of nozzle size and position used in the experiment. Using Eq. (1) it is possible to express the decay in alignment due to collisions as a depolarization. The polarization that would be measured in the absence of second collisions may then be expressed in terms of the polarization after the effect of the collisions, $P_{sc}(t_d)$ to give

$$P=\frac{3P_{sc}(t_d)}{3\exp(-\gamma_c^{(2)}t_d)+[1-\exp(-\gamma_c^{(2)}t_d)]P_{sc}(t_d)}. \tag{5}$$

In this correction we are making the assumption that the pulse widths are small compared with the delay. This is obviously not valid for the small delays that have been used. However, the fact that all the data shown in Fig. 3 can be well fitted to a straight line, as expected from Eq. (4), leads us to believe that Eq. (5) may be safely used to correct the data for the effects of collisions. There is also the fact that all of the polarization data we present was taken using a small delay (4.5 ns) and the actual correction that has to be applied to the data is in all cases small. As a result the errors introduced by this correction method do not significantly increase the size of the error bars which are, in fact, dominated by shot noise.

III. INTERATOMIC POTENTIALS

As previously mentioned, one of the original motivations for choosing to work in the Hg–Ar system is that much work has been carried out on the interatomic potentials. Petzold *et al.*[10] have performed temperature dependent line shape measurements and Fuke *et al.*[8] performed spectroscopy on cold van der Waals molecules in a system identical to our own. The potentials originally used in the simulations[13] were those of Segal and Harris[12] and were based on the Morse potentials of Fuke *et al.* Comparisons of our vibrational spectra with those of Fuke *et al.* revealed discrepancies in the positions of the bound–bound vibrational peaks and in the dissociation energy for dissociation from the ground vibrational state to the continuum on the excited B state potential. This was measured to be 132 cm^{-1} by Fuke *et al.* and 123.5 cm^{-1} by us. We performed a separate test of the frequency calibration of our lasers by measuring the bound–bound spectra for Hg–Kr van der Waals molecules. These agreed within our experimental error of ± 0.2 cm^{-1} with the positions of these lines measured by Yamanouchi *et al.* using a narrow linewidth laser and so we are confident that our lasers were correctly calibrated. These discrepancies in the positions of the peaks, and the resulting errors in the potentials, were enough to make any comparisons of our polarization data with results from models using these potentials meaningless, particularly given the large error in the dissociation energy which is critical to correct predictions of the polarizations. It was therefore decided to construct our own potentials from the spectroscopic data gathered from our experiment.

In a supersonic jet, it is the lowest vibrational level in the ground state that is predominantly populated. Consequently, the fluorescence excitation spectrum of the cooled molecule becomes extremely simple as demonstrated by the spectrum shown in Fig. 4. Two groups of bands were observed, one in the lower and one in the higher frequency region of the Hg atomic line center (39 412 cm^{-1}). The former group of bands corresponds to transitions from the ground state to the excited A state and the latter to transitions from the ground state to the excited B state. Table I summarizes the band positions observed in this experiment. For both sets of bands a Birge–Sponer plot of the variation of $\Delta G_{v'+1/2}$ with v' is linear over the whole range of each band (Fig. 5). This suggests that parametrizing the potentials as Morse potentials (as was done by both Fuke *et al.* and Yamanouchi *et al.*) provides a reasonably accurate approximation to the true interatomic potentials. However, the Morse potential suffers from the drawback that it converges to zero too quickly for a correct description of the long-range $1/R^6$ van der Waals interaction. We therefore follow the prescription of Segal and Harris[12] and use hybrid potentials based on the Morse potentials of Fuke *et al.* and $1/R^6$ potentials given by Ben Lakhdar *et al.*[11] joined at intermediate R. From the data we had we were able to derive new Morse potential parameters for the excited A and B states from the Birge–Sponer plots and also to give a new value of the depth D_e of the ground state potential. We were, however, not able to perform a dispersed fluorescence experiment and could not determine the remaining ground state parameters and the values for the internuclear separations. We have therefore used the values given by Fuke *et al.* for these parameters. The new potentials used are summarized in Table II.

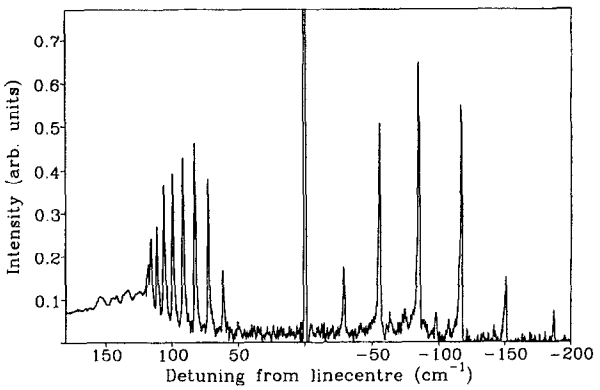

FIG. 4. Single photon fluorescence excitation spectrum of the Hg–Ar van der Waals molecules. Plotted as a function of detuning from the Hg($6s\ ^1S_0$–$6p\ ^3P_1$) line center.

IV. RESULTS AND DISCUSSION

The variation of polarization with detuning is shown in Fig. 6 for the four different beam temperatures for which the experiment was performed. All points have been corrected for secondary depolarizing mechanisms and the er-

TABLE I. Assignments and positions of the observed bands in the A–X and B–X transitions of Hg–Ar.

$A\ ^3\Omega^+$–$X\ ^1\Omega^+$		$B\ ^3\Pi_1^+$–$X\ ^1\Omega^+$	
$v'-v''$	ν_{em} (cm^{-1})	$v'-v''$	ν_{em} (cm^{-1})
1–0	39 224.3	0–0	39 474.1
2–0	39 261.5	1–0	39 485.5
3–0	39 295.5	2–0	39 495.5
4–0	39 327.1	3–0	39 504.4
5–0	39 356.3	4–0	39 512.1
6–0	39 383.0	5–0	39 518.8
		6–0	39 524.1
		7–0	39 528.3
		8–0	39 531.3
		9–0	39 533.3

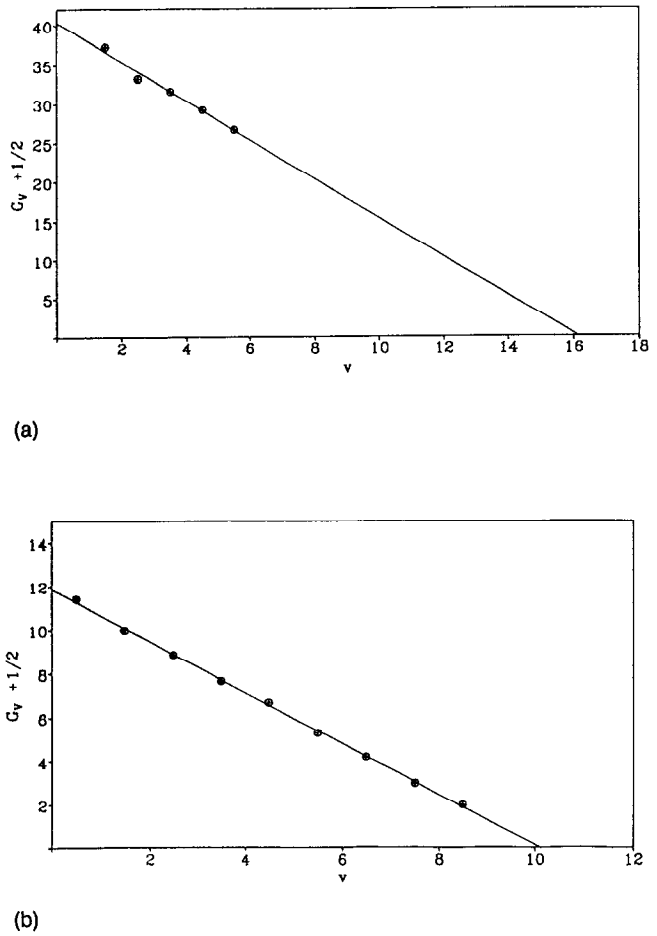

FIG. 5. Birge–Spooner plots of $\Delta G_{v+1/2}$ vs v for (a) A and (b) B states of Hg–Ar.

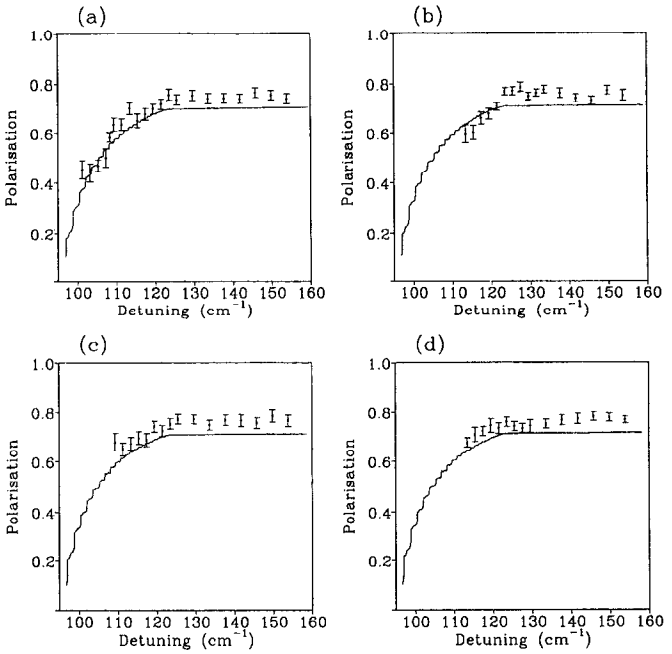

FIG. 6. Polarization data for the four expansion temperatures studied. Shown with the polarizations predicted from the simulations (solid line). Plotted as a function of detuning from the Hg($6s\ ^1S_0$–$6p\ ^3P_1$) line center. (a) 350 μm nozzle probed at 2 mm, (b) 350 μm nozzle probed at 5 mm, (c) 150 μm nozzle probed at 2 mm, and (d) 150 μm nozzle probed at 5 mm.

ror bars shown in Fig. 6 are a combination of the statistical error on the data and the errors arising from the correction process. Close to threshold the effects of very low signal on the statistical error has been somewhat offset by the acquisition of more data for these points. In all cases the results show a qualitative agreement with the variation in polarization expected from a sudden decoupling picture of the process. The polarization close to threshold is reduced, due to the fragments separating slowly, allowing more time for rotation, and then shows a definite rise once the dissociation limit has been passed, and in all cases tends to the same limiting value of $\sim 78\%$ for high photon energies. This high polarization is called the recoil limit since it occurs when the pair dissociates without any rotation of the internuclear axis. Consequently there is no reorientation, i.e., rotation of the dipole as the molecule dissociates. This will be the case either when the molecule is in a very low J_i rotational state or when the pair separates very quickly, i.e., with high kinetic energy. Further the level of polarization close to threshold is considerably lower for the cases where the beam temperature is higher. In the high temperature cases we have also been able to take data at detunings lower than the dissociation limit for the $J_i=0$ state. This is because at these temperatures a significant number of higher rotational J_i states will be thermally populated, having the effect of shifting the onset of the dissociation continuum to slightly lower frequencies.

TABLE II. Summary of the hybrid potential parameters.

State	ϵ/cm^{-1}	ω_e/cm^{-1}	$\omega_e x_e/cm^{-1}$	r_m/Å	C_6/cm^{-1} Å^6	C_8/cm^{-1} Å^8
$X\ ^1 0^+$	135.2	23.5	1.06	4.01	5.63×10^5	8.71×10^6
$A\ ^3 0^+$	371.3	41.6	1.25	3.38	8.45×10^5	6.02×10^5
$B\ ^3 1$	72.02	12.4	0.59	4.66	1.28×10^6	9.74×10^6

Comparison with a QM calculation for the system

This shift of the dissociation continuum to lower energies with higher J_I has allowed us to make an estimate of the rotational temperature of the beam. This was done by comparing the shape of the dissociation continuum with the total cross section for dissociation calculated from our quantum mechanical calculations for the system by assuming a Boltzmann distribution. The calculation itself utilizes a time dependent wave-packet propagation method[13] where the initial wave packet from the lower electronic vibrational state is projected onto the excited electronic state manifold and evolved out to large internuclear separation. These comparisons are shown in Fig. 7 together with estimates for the temperatures for each of the cases for which data was taken. This method was found to be quite sensitive allowing the temperatures to be estimated to an accuracy of 0.2 K. The variation in temperature over

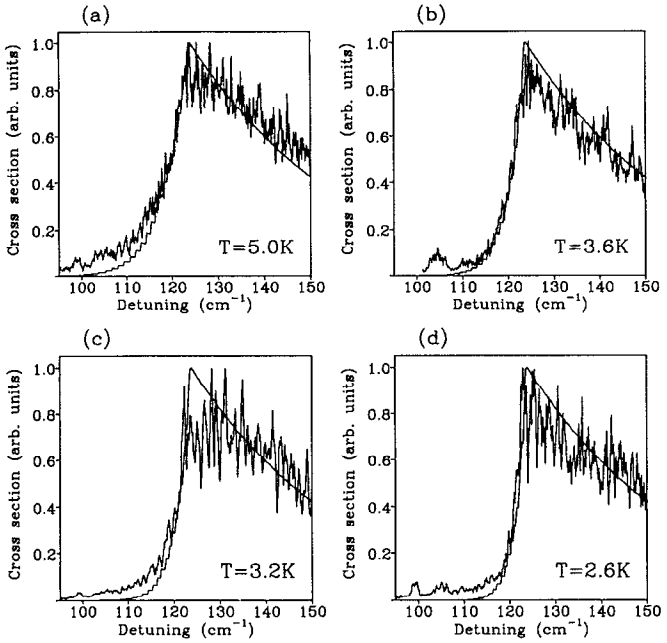

FIG. 7. Total dissociation cross section measured experimentally for the four beam temperatures together with predicted cross sections calculated from the QM calculations, plotted as a function of detuning from the Hg($6s\ ^1S_0$–$6p\ ^3P_1$) line center. The temperatures given are those that gave the best agreement between the predicted and measured cross sections. (a) 350 μm nozzle probed at 2 mm, (b) 350 μm nozzle probed at 5 mm, (c) 150 μm nozzle probed at 2 mm and, (d) 150 μm nozzle probed at 5 mm.

the four cases is as expected but the absolute values are all somewhat higher that those predicted by continuum mechanics. This higher than expected temperature agrees with that measured by Yamanouchi *et al.* (see Sec. II B), who measured the temperature by rotationally resolving the vibrational structure. This method was not, however, available to us due to the larger bandwidth of our laser. An estimation of the beam rotational temperature is essential if we are to compare the experimental polarization results with the polarizations predicted by the calculations. This is because to obtain an accurate comparison with the experimental data, the theoretical results have to be thermally averaged over all the J_i states populated in the expansion. The results of the model are shown in Fig. 6 together with the experimental results.

The comparison shows that close to or below the $J_i=0$ threshold the polarizations are predicted with reasonable accuracy. At higher photon energies (detunings greater than the $J_i=0$ dissociation threshold) the polarizations are, however, typically 5% higher than those predicted by the model. The polarizations measured in this region were in the range 76%–78%, very close to the theoretical maximum, the recoil limit, of 78%. There are two possible reasons for this modest discrepancy in the polarization level. The first, and most likely, is that the long-range part of the potential is not particularly accurate. The polarization is most sensitive to this region of the potential because the decoupling from molecular states to atomic states depends critically on the A and B state separation. Consequently, the lower polarizations predicted by the model could be explained by the potentials, giving a larger decoupling radius than actually exists. The second reason may lie in the treatment of the effects of the hyperfine structure. In the quantum mechanical calculations hyperfine structure is not taken into account. The correction that therefore has to be applied to the experimental data assumes that all the hyperfine recoupling occurs after dissociation has taken place and the atom has become fully asymptotic. However, the time over which the hyperfine recoupling takes place is of order 50 ps and a typical dissociation time is about 10 ps, so it is possible that some discrepancies will arise due to partial recoupling to the hyperfine states during dissociation. Given that the total hyperfine correction is small, however, it is unlikely that this effect could account for all of the observed discrepancy in the polarizations.

V. CONCLUSIONS

We have applied a sensitive technique for monitoring the asymptotic alignment of Hg atoms to the case of photodissociation of Hg–Ar van der Waals molecules. This has allowed us to conduct a very clean near threshold dissociation experiment free from depolarization processes, such as radiation trapping, which are very hard to correct for. The polarization of the asymptotic atoms has, for the first time to our knowledge, been measured as a function of dissociating energy from very close to threshold, corresponding to cold half-collisions with slow moving particles, to higher photon energies where the photofragments move apart with some speed. The polarization results compare well with what would be expected from locking pictures, again confirming the usefulness of these simple pictures in interpreting collision processes. For comparison with the quantum mechanical calculations new potentials have been suggested in the form of a hybrid between a Morse potential and a long-range van der Waals interaction. Polarization predictions based on these new potentials were in good agreement for dissociation close to threshold, but the slight disagreements for high recoil energies suggest that more work is needed on the very long-range parts of the potentials.

The fact that the theory predicts the level of polarization quite well, particularly close to threshold, is most encouraging. Now that the technique has been proven to work we intend to use it for the study of collision dynamics down to far lower temperatures than the few kelvin presently accessible in this experiment. Use of narrow a linewidth cw laser will allow us to probe much closer to the dissociation threshold of a particular state than is currently possible. The use of Raman pumping of specific initial rovibrational states would also allow the preparation and dissociation of a single J_i initial state. This should enable us to probe the long-range forces that influence very cold, slow moving, atoms and hence examine the collisional interaction that determines the behavior of atoms in laser cooled and trapped gases with unprecedented selectivity and accuracy.

ACKNOWLEDGMENTS

We wish to thank the U.K. Science and Engineering research Council for supporting this work and for the award of studentships to C.J.K.Q. and I.M.B., the Run Run Shaw Foundation for the award of a Run Run Shaw scholarship (X.C.), and the Soros Foundation for the award of a Soros/FCO scholarship (E.T.).

[1] V. Zafiropulos, P. D. Kleiber, K. M. Sando, X. Zeng, A. M. Lyra, and W. C. Stwalley, Phys. Rev. Lett. **61**, 1485 (1988).
[2] P. D. Kleiber, J. X. Wang, K. M. Sando, V. Zafiropulos, and W. C. Stwalley, J. Chem. Phys. **95**, 4168 (1991).
[3] R. L. Dubs and P. S. Julienne, J. Chem. Phys. **95**, 4177 (1991).
[4] M. Glass-Maujean and J. A Beswick, Phys. Rev. A **36**, 1170 (1987).
[5] S. R. Leone, Acc. Chem. Res. **25**, 71 (1992).
[6] E. L. Lewis, M. Harris, W. J. Alford, J. Cooper, and K. Burnett, J. Phys. B **16**, 553 (1983).
[7] I. V. Hertel, H. Schmidt, A. Bahring, and E. Mayer, Rep. Prog. Phys. **48**, 375 (1985).
[8] K. Fuke, T. Saito, and K. Kaya, J. Chem. Phys. **18**, 2591 (1984).
[9] K. Yamanouchi, S. Isogai, M. Okunishi, and S. Tsuchiya, J. Chem. Phys. **88**, 205 (1988).
[10] H. C. Petzold and W. Behmenberg, Z. Naturforsch. Teil A **33**, 1461 (1978).
[11] Z. Ben Lakhdar, D. Perrin, and R. Lennuier, J. Phys. **37**, 831 (1976).
[12] D. Segal and I. D. Harris, J. Chem. Phys. **94**, 2713 (1991).
[13] X. Chen, K. Burnett, and D. M. Segal, J. Chem. Phys. **95**, 8124 (1991).
[14] I. M. Bell, C. J. K. Quayle, D. M. Segal, and K. Burnett, Phys. Rev. A **47**, 3128 (1993).
[15] M. G. Littman and H. J. Metcalf, Appl. Opt. **14**, 2224 (1978).
[16] D. R. Miller, in *Atomic and Molecular Beam Methods*, edited by G. Scoles (Oxford University Press, New York, 1988).
[17] U. Fano and J. H. Macek, Rev. Mod. Phys. **45**, 553 (1972).
[18] I. C. Percival and M. J. Seaton, Philos. Trans. R. Soc. London Ser. A **251**, 113 (1958).
[19] J. Macek and I. V. Hertel, J. Phys. B **7**, 2173 (1974).
[20] I. V. Hertel and W. Stoll, Adv. Atom. Mol. Phys. **13**, 113 (1978).
[21] C. H. Greene and R. N. Zare, J. Chem. Phys. **78**, 6714 (1983).
[22] I. M. Bell, C. J. K. Quayle, and K. Burnett (in preparation).
[23] A. Omont, J. Phys. **26**, 26 (1965).
[24] W. J. Alford, N. Andersen, K. Burnett, and J. Cooper, Phys. Rev. A **30**, 2366 (1984).
[25] D. M. Segal and K. Burnett, J. Chem. Soc. Faraday Trans. 2 **85**, 925 (1989).